Antitumor Activity of MEDI3726 (ADCT-401), a Pyrrolobenzodiazepine Antibody-drug Conjugate Targeting PSMA, in Pre-clinical Models of Prostate Cancer

Song Cho[1*], Francesca Zammarchi[2*], David G. Williams[3], Carin E.G. Havenith[2], Noel R. Monks[1], Peter Tyrer[3], Francois D'Hooge[3], Ryan Fleming[1], Kapil Vashisht[1], Nazzareno Dimasi[1], Francois Bertelli[3], Simon Corbett[3,4], Lauren Adams[3], Halla W. Reinert[4], Sandamali Dissanayake[2], Charles E. Britten[2], Wanda King[1], Karma Dacosta[1], Ravinder Tammali[1], Kevin Schifferli[1], Patrick Strout[1], Martin Korade III[1], Mary Jane Masson Hinrichs[1], Simon Chivers[2], Eva Corey[5], He Liu[6], Sae Kim[6], Neil H. Bander[6], Philip W. Howard[3], John A. Hartley[3,4], Steve Coats[1], David A. Tice[1], Ronald Herbst[1], Patrick H. van Berkel[2].

* Song Cho and Francesca Zammarchi are co-first authors

Author Affiliations: [1]MedImmune, Gaithersburg, US; [2]ADC Therapeutics SA, Epalinges, Switzerland; [3]Spirogen, London, United Kingdom; [4]University College London, London, United Kingdom; [5]University of Washington, Seattle, US; [6]Department of Urology,Weill Cornell Medical College-NewYork Presbyterian Hospital, New York, US.

Running Title: MEDI3726 is a novel ADC targeting PSMA

Key Words: MEDI3726 (ADCT-401), antibody-drug conjugate, prostate-specific membrane antigen, pyrrolobenzodiazepine dimer

Disclosure of Potential Conflicts of Interest:

MedImmune authors are employees of MedImmune and may have ownership interest in AstraZeneca/MedImmune. Spirogen authors are employees of Spirogen/MedImmune and may have ownership interest in MedImmune. F. D'Hooge is the Head of the Bioconjugation Unit at Novasep. P.W. Howard has ownership interest (including patents) in ADC Therapeutics. P.H.C. van Berkel has ownership interest (including patents) in ADC Therapeutics. ADC Therapeutics authors are employees of ADC Therapeutics. J.A. Hartley reports receiving a commercial research grant from, has ownership interest (including patents) in, and is a consultant/advisory board member for ADC Therapeutics. All other ADC Therapeutics affiliated authors are ADC Therapeutics employees. Dr. Bander is an inventor on patents related to the J591 anti-PSMA antibody that are assigned to Cornell Research Foundation ("CRF"). Dr. Bander is a paid consultant to and owns equity in BZL Biologics, LLC, the company to which the patents were licensed by CRF for further research and development. No potential conflicts of interest were disclosed by the other authors.

Corresponding Authors:

Song Cho
Senior Scientist, Oncology Research
MedImmune
One MedImmune Way
Gaithersburg, MD 20878
Phone: 301-398-5667
Email: chos@medimmune.com

Francesca Zammarchi
Senior Cancer Biologist
ADC Therapeutics
42 New Road, E1 2AX, London, U.K.
Email: francesca.zammarchi@adctherapeutics.com

Abstract Word Count: 200
Manuscript Word Count: 4999
Total Number of Figures/Tables: 6
Total Number of Supplemental Figures/Tables: 11
References: 44

ABSTRACT

Prostate specific membrane antigen (PSMA) is a membrane bound glutamate carboxypeptidase that is highly expressed in nearly all prostate cancers with the highest expression in metastatic castration-resistant prostate cancer (mCRPC). The prevalence of increased surface expression and constitutive internalization of PSMA make it an attractive target for an antibody-drug conjugate (ADC) approach to treating patients with mCRPC. MEDI3726 (previously known as ADCT-401) is an ADC consisting of an engineered version of the anti-PSMA antibody J591 site-specifically conjugated to the pyrrolobenzodiazepine (PBD) dimer tesirine. MEDI3726 specifically binds the extracellular domain of PSMA and, once internalized, releases the PBD dimer to crosslink DNA and trigger cell death. In vitro, MEDI3726 demonstrated potent and specific cytotoxicity in a panel of PSMA-positive prostate cancer cell lines, consistent with internalization and DNA interstrand crosslinking. In vivo, MEDI3726 showed robust antitumor activity against the LNCaP and the castration-resistant CWR22Rv1 prostate cancer cell line xenografts. MEDI3726 also demonstrated durable antitumor activity in the PSMA-positive human prostate cancer patient-derived xenograft (PDX) LuCaP models. This activity correlated with increased phosphorylated Histone H2AX in tumor xenografts treated with MEDI3726. MEDI3726 is being evaluated in a Phase 1 clinical trial as a treatment for patients with metastatic castrate-resistant prostate cancer (NCT02991911).

INTRODUCTION

In the United States, prostate cancer is the most common cancer and the third leading cause of cancer deaths in men, with an estimated 161,360 new cases annually (1). Patients with metastatic prostate cancer initially respond to androgen deprivation therapy, but nearly all develop castration resistant disease (2). Although recent therapeutic advances provide a survival benefit, not all patients respond, and those who do respond eventually develop resistance and experience disease progression (3). Therefore, there is a need for improved therapies for patients with metastatic castration-resistant prostate cancer (mCRPC).

Prostate specific membrane antigen (PSMA), also known as glutamate carboxypeptidase II, has two known enzymatic functions. In the small intestine, it removes glutamates from dietary folates for absorption, and in the central nervous system, it hydrolyzes the most prevalent peptidic neurotransmitter, N-acetylaspartylglutamate (4). PSMA is also expressed in renal tubule epithelium and normal prostate tissue, although the function of PSMA in these tissues is not well understood (4). In contrast to the limited normal tissue expression at sites not accessible to an intact antibody (5), PSMA is highly expressed in the epithelium of nearly all primary and metastatic prostate cancers (6-9) and in the neovasculature that supplies most non-prostatic solid tumors, including carcinomas of the lung, colon, breast, kidney, liver, and pancreas as well as sarcomas and melanoma (10,11). It is a clinically validated tumor-associated antigen for imaging prostate cancer, and PSMA-targeted anti-cancer therapies involving multiple modalities have demonstrated early signs of clinical activity (12-18).

Antibody drug conjugates (ADCs) consist of antibodies that specifically target tumor-associated antigens and are conjugated to small molecules that possess strong cytotoxic activity (19). Among the most potent cytotoxins are pyrrolobenzodiazepine (PBD) dimers, which can form highly cytotoxic DNA interstrand crosslinks (ICL) (20). Because the crosslinks formed by PBD dimers are relatively non-distorting of the DNA structure, PBD dimer crosslinks are less susceptible to DNA repair mechanisms (21). Several ADCs are under clinical evaluation in both hematologic and solid tumor indications employ PBD dimers; e.g. rovalpituzumab tesirine and

vadastuximab talirine are in phase 3 studies in small cell lung cancer and acute myeloid leukaemia, respectively (22).

MEDI3726 (formerly known as ADCT-401, Figure 1), is a PSMA-targeting ADC generated via site-specific conjugation of an engineered version of the anti-PSMA deimmunized (humanized) immunoglobulin G1 (IgG1) κ antibody J591 (23) to the PBD-based linker-drug tesirine (SG3249), which is the same PBD dimer used in rovalpituzumab tesirine (24). MEDI3726 is under evaluation in a phase 1 clinical trial as an anticancer treatment in patients with mCRPC (NCT02991911). Herein we describe the in vitro and in vivo characterization of MEDI3726.

MATERIALS AND METHODS

Generation of ADCs

The antibody component of MEDI3726, J591, and the non-PSMA–targeting isotype control ADC contain the mutations C214S in the light chain and C226V and C229V in the heavy chain hinge (antibody numbering herein is according to EU numbering) (25). These mutations allow the site-specific conjugation of maleimide at position C220 with the drug linker tesirine. The conjugation procedure and the analytical characterization of MEDI3726 as well as the generation and purification of the soluble recombinant extracellular PSMA domains (sPSMA) for human (shPSMA), cynomolgus monkey (*Macaca fascicularis*, scPSMA), and rat (srPSMA) are described in the Supplementary Methods section.
Two monomethyl auristatin E (MMAE)-based ADCs targeting PSMA (PSMA-ADC1-MMAE and PSMA-ADC2-MMAE) were generated as described in patent US 8114965 B2 by Concortis (San Diego, USA).

Competitive ELISA to Determine Species Cross-Reactivity

The ability of each sPSMA to displace MEDI3726 from shPSMA was determined by competitive ELISA. Briefly, Maxisorp microplates (Nunc) were coated with shPSMA (50 μL/well, 1.0 μg/mL in PBS) and incubated at 4°C overnight. A 2-fold dilution series of each

sPSMA antigen was dispensed (50 μL/well, in PBS/Tween/BSA (PBS 0.05%, Tween 20 (v/v), 2% BSA (w/v)). MEDI3726 was then added (50 μL / well of 0.2 μg/mL in PBS/Tween/BSA) and incubated for 1 h at room temperature (RT). After the MEDI3726-shPSMA complex was washed, 50 μL of goat antihuman immunoglobulin G (IgG)-horseradish peroxidase (HRP) conjugate (Jackson Immunoresearch) (diluted 1:1000 in PBS/Tween/BSA) was added and incubated for 1 h at RT. After the wash, TMB-Turbo (Thermo Fisher Scientific) was added (75 μL/well) and the reaction was stopped with hydrochloric acid (HCl) (75 μL/well, 0.6 M). Well optical densities were measured on the EnVision plate reader (PerkinElmer) at 450 nm and data were analyzed by using GraphPad Prism (GraphPad Software, Inc.).

In Vitro Characterization of PSMA Expression and MEDI3726 Activity

The LNCaP, CWR22Rv1, MDA PCa 2b, PC-3, and DU145 prostate cancer cell lines were obtained from American Type Culture Collection (ATCC) and maintained by following ATCC recommendations. The authentication of these mycoplasma negative lines was performed by ATCC to verify the identity of human cell lines and to rule out both intra- and interspecies contamination. The cell lines used in the assays were not re-authenticated or tested at ADC Therapeutics, but they were passaged for fewer than 6 months after the initiation of culture. The LNCaP C4-2 cell line was a gift from Dr. Neil Bander (Weill-Cornell Medical College). Upon arrival, the cell line went authenticity and IMPACT testing (for murine viruses) by IDEXX Bioresearch. Cell surface PSMA expression and antigen density were quantitated by flow cytometry on a panel of six human prostate cancer cell lines including LNCaP, LNCaP C4-2, CWR22Rv1, MDA PCa 2b, PC-3, and DU145. The specific antigen density for each cell line was calculated by using Quantum Simply Cellular Anti-Human IgG beads (Bangs Laboratories) according to the manufacturer's instructions, with the antibody component of MEDI3726. The percentage of PSMA-positive cells in the prostate cancer cell lines was calculated from the MFI (mean fluorescence intensity) of each cell line, based on the same data set, by using FlowJo v10 (FlowJo, LLC) for analysis.

The cytotoxic activity was determined by CellTiterGlo. The cell suspension was diluted to the required seeding density (generally 10^5/mL), dispensed into white 96-well flat-bottomed

microplates (50 μL/well), and incubated overnight. Eight 10-fold serial dilutions of ADCs or SG3199 (the warhead component of tesirine) were dispensed (50 μL/well) into 4 replicate wells of a 96-well plate containing cells. Control wells received culture medium (50 μL/well) only. The cytotoxicity of SG3199, MEDI3726, and the non-targeted isotype control ADC was measured in each cell line after an incubation period ranging from 5 to 7 days at 37°C and 5% carbon dioxide. This incubation period was calculated to be at least three normal cell doubling times and was used for exposure to either warhead toxin or ADCs. After the ADC exposure period, cell viability was measured with the CellTitreGlo assay (Promega) following the manufacturer's protocol. IC_{50} values were calculated by using GraphPad to fit luminescence data to a sigmoidal dose-response curve with variable slope.

MEDI3726 Internalization and Lysosomal Trafficking

Immunofluorescence microscopy was used to detect internalization and colocalization of MEDI3726 or an isotype control ADC with the lysosomal marker, lysosome-associated membrane protein 1 (LAMP1). One cell line demonstrated to be PSMA positive and one demonstrated to be PSMA negative were incubated with MEDI3726 or the isotype control ADC. A detailed protocol is provided in the Supplementary Methods.

Single Cell Gel Electrophoresis (Comet) Assay

The modified single-cell gel electrophoresis (Comet) assay as described by Hartley et al (26) was used to monitor the formation of DNA ICLs generated by the SG3199, MEDI3726, or the non-targeting isotype control ADC and the unhooking step of repair of these ICLs. Briefly, 10^5 cells were seeded in 24-well plates and treated with MEDI3726 (6 nM), isotype control ADC (4.7 nM, an equimolar PBD concentration) or SG3199 (2.5 nM) for 2 h, washed, and incubated with drug-free culture medium for the required posttreatment time (up to 36 h). At each time point, cells were harvested and stored at -80°C until they were used. Except for non-irradiated controls, thawed samples ($3x10^4$ cells/mL) were irradiated (15 Gy) to introduce a fixed number of random DNA strand breaks and then processed for the Comet assay. The Olive Tail Moment (OTM) was determined as described previously (27), using the formula:

$$\% \text{ decrease in OTM} = (1-(TMdi-TMcu/TMci-TMcu)) \times 100$$

where *TMdi* is the tail moment of drug-treated, irradiated sample; *TMcu* is the tail moment of untreated, non-irradiated control; and *TMci* is the tail moment of untreated, irradiated control. Crosslinking was expressed as the percentage decrease in the OTM compared with control irradiated cells.

Determination of the In Vivo Activity of MEDI3726 in LNCaP, CWR22Rv1, and PC-3 Xenograft Models

The LNCaP xenograft study was performed by Crown Bioscience, United Kingdom, according to ethical standards and practice. LNCaP cells ($5x10^6$) were implanted subcutaneously with Matrigel (1:1) (BD Biosciences) into the left flank of 4-8 week old male MF1 nude mice (Hsd:Ola-MF1-Foxn1nu, Envigo, UK). Once the mean tumor volume reached ~200 mm^3, animals were randomized (based on tumor volume) into study groups (n=10), and dosing with ADCs was initiated (Day 1). The body weight of mice ranged from 22.6 g to 35.3 g. Each animal was euthanized when its tumor attained the endpoint tumor volume of 1,700 mm^3 or on the final day (Day 64), whichever came first.

The CWR22Rv1 (a castration-resistant prostate cancer model (28)) and PC-3 studies were completed at Charles River Discovery Services (Morrisville, NC), in an Association for Assessment and Accreditation of Laboratory Animal Care (AAALAC) accredited facility in compliance with accepted standards for the care and use of laboratory animals. CWR22Rv1 cells (1×10^7), were implanted subcutaneously with Matrigel (1:1) in the right flank of male C.B-17 SCID mice (Fox Chase SCID, C.B-17/Icr- Prkdcscid/IcrIcoCrl, Charles River). When the mean tumor volume reached ~120 mm^3, animals were randomized (based on tumor volume) into study groups (n=10) and treatment was initiated (Day 1). Mice were ten weeks old with a body weight range of 18.6 g to 27.2 g on Day 1 of the study. For the PC-3 xenograft study, 1 mm^3 tumor fragments were implanted subcutaneously in the right flank of each female athymic nude mouse (Crl:NU(Ncr)-Foxn1nu, Charles River). When the mean tumor volume reached ~135 mm^3, mice

were randomized (based on tumor volume) into study groups (n=10) and the treatment was initiated (Day 1). Mice were eleven weeks old with a body weight range of 17.5 g to 27.6 g on Day 1 of the study. In the CWR22Rv1 and PC-3 studies, each animal was euthanized when its tumor volume exceeded 1,000 mm^3, or on the final day (Day 94 for the CWR22Rv1 study and Day 60 for the PC-3 study), whichever came first.

All dosing materials were administered intravenously as a single dose except for the MMAE-based PSMA-targeted ADCs, which were administered once every 4 days for six doses total. Both tumor and body weight measurements were collected twice weekly, and the tumor volume was calculated using the formula:

$$\text{tumor volume } (mm^3) = [\text{length (mm)} \times \text{width (mm)}^2]/2.$$

Statistical analysis is described in the Supplementary Methods.

Determination of In Vivo Activity of MEDI3726 in LuCaP PDX Models

The LuCaP 35CR, 58, 70, 73, 77, 86.2, 96CR and 147 prostate cancer PDX models were used (29). LuCaP 35CR and LuCaP 96CR are castration-resistant models established and maintained in castrated male mice (29). All LuCaP models used in this study express differing levels of androgen receptor (AR) splice variant AR-V7, and LuCaP 86.2 model expresses the AR-V567es variant (30,31).

The general health of the mice was monitored daily, and all experiments were conducted in an AAALAC-accredited facility in accordance with MedImmune's Institutional Animal Care and Use Committee guidelines for humane treatment and care of laboratory animals. All PDX models were maintained in-life by continuous passage in 8- to 12-week-old male C.B-17/IcrHsd-*Prkdc*^{scid} mice (Envigo). Both the LuCaP 35CR and 96CR models were propagated in castrated male mice. To initiate tumor growth, 3 mm^3 tumor fragments were implanted subcutaneously into the right flank of 8- to 12-week-old male C.B-17/IcrHsd-*Prkdc*^{scid} mice (Envigo) by using an 11-gauge trocar needle. Once the tumors reached a size of 150 to 250 mm^3, the mice were

randomized (based on tumor volume) into study groups of 6 mice per group. The body weight of mice ranged from 21.1 g to 25.5 g at the initiation of dosing. MEDI3726 was given intravenously at doses of 0.1, 0.3, or 0.9 mg/kg, and the isotype control ADC was given at a dose of 0.9 mg/kg. Both ADCs were administered intravenously once every 3 weeks for three doses according to body weight. Tumor and body weight measurements, and the statistical analysis were carried out as described above.

Immunohistochemistry of Tumor Xenografts

Detailed immunohistochemistry (IHC) protocols for detecting PSMA and phosphorylated Histone H2AX (γ-H2AX) and the quantification of γ-H2AX are provided in the Supplementary Methods. Briefly, the PSMA IHC assay used mouse monoclonal anti-human PSMA clone 3E6 (Dako) and mouse IgG1 isotype control (R&D System), and was performed on the Dako autostainer by using the Dako EnVision+ System-HRP (DAB) Kit. For the γ-H2AX IHC, LuCaP 73 xenograft-bearing animals were dosed once, and xenograft tumors were collected 48 h after the dose for formalin-fixed paraffin-embedded generation. The rabbit anti-γ-H2AX (Ser139) (20E3) (Cell Signaling Technology) was used on the Ventana Discovery ULTRA Staining Module. Stained slides were scanned with the Aperio Scanscope AT Turbo for the generation of digital images, and γ-H2AX-positive nuclei were quantified by using Aperio Nuclear Algorithm. Statistically significant differences were determined by using one-way ANOVA with posthoc Tukey for the multiple comparison. GraphPad Prism 7 was used for statistical analyses.

RESULTS

MEDI3726

MEDI3726 had a monomer content of 98% as determined by size-exclusion chromatography (SEC) and a drug to antibody ratio (DAR) as measured by reduced liquid chromatography mass spectrometry (LCMS), close to 2. Both shPSMA and scPSMA competed for binding of MEDI3726 to shPSMA with similar half-maximal effective concentrations of 17.92 ng/mL and 16.89 ng/mL, respectively (Table 1). However, srPSMA did not compete for binding to

MEDI3726, indicating a lack of rodent cross-reactivity for J591. As demonstrated by surface plasmon resonance, MEDI3726 bound to shPSMA and scPSMA with similar affinities of 1.67 nM and 3.11 nM, respectively, consistent with the competitive ELISA data (Table 1). MEDI3726 maintained activity for up to 7 days in PBS or human or cynomolgus monkey plasma at 37°C as determined by in vitro cytotoxic activity on LNCaP cells, binding to sPSMA and determination of PBD containing ADC by anti-PBD antibody capture assays (Supplementary Figure S1).

In Vitro Characterization of PSMA Expression and Activity of MEDI3726

The LNCaP and LNCaP C4-2 prostate cancer lines had the highest antigen densities, whereas PC-3 and DU145 had antigen densities below the lower limit of quantitation (7,348) for the assay and were therefore classified as PSMA-negative (Table 2). More than 90% of LNCaP, LNCaP C4-2, and MDA PCa 2b cells were positive for PSMA expression, but fewer than half of the CWR22Rv1 cells were PSMA-positive (Table 2).

SG3199, the warhead component of tesirine, displayed potent cell-killing activity in all cell lines (IC_{50} ranging from 0.04 nM to 1.05 nM). Target specific cytotoxicity of MEDI3726 was observed in the four PSMA-positive cell lines (LNCaP, LNCaP C4-2, MDA PCa 2b, and CWR22Rv1). For the two PSMA-negative cell lines, the IC_{50} ratio of the isotype control ADC to MEDI3726 was approximately 1, indicating that no targeted cytotoxicity occurred in cell lines lacking PSMA expression (Table 2).

Internalization and DNA Crosslinking

Cellular internalization and trafficking of MEDI3726 to the lysosome are essential for SG3199 to be released from other tesirine components by cleavage of the valine-alanine dipeptide linker. Within 24 h of continuous ADC exposure, MEDI3726 was internalized and trafficked to LAMP-1-positive lysosomes in PSMA-positive LNCaP cells (Figure 2A). Conversely, MEDI3726 was not internalized by the PSMA-negative PC-3 cells, indicating that uptake of MEDI3726 was

specific to PSMA (Figure 2B). The isotype control ADC did not bind and was not internalized by LNCaP or PC-3 cells (Figures 2C and 2D, respectively).

Immediately after LNCaP cells were incubated with MEDI3726, a low level of DNA crosslinking (5%) was observed and increased with time to a peak level of approximately 50% at 24 h, which persisted at 36 h (Figure 2E). SG3199 induced ICLs more rapidly, with approximately 35% observed at the end of the incubation period and a peak of more than 60% by 6 h. Peak level of crosslinking induced by SG3199 also persisted at 36 h. The lower level of and longer time to maximum ICL formation by MEDI3726 likely arose from differential uptake and an extra processing hurdle of MEDI3726 to release the payload compared to SG3199 which can diffuse across the membrane and crosslink DNA without processing.

In the PSMA-negative cell line PC-3, MEDI3726 did not produce a significant level of DNA ICLs over 36 h (Figure 2F). However, SG3199 produced a high level of ICLs, similar to that observed in the LNCaP cell line. These results are consistent with the target-mediated internalization and cell killing by MEDI3726.

In Vivo Activity of MEDI3726 in Prostate Cancer Cell Line Xenografts

As determined by IHC, PSMA expression in the LNCaP xenografts was homogeneous, with nearly all tumor cells staining strongly positive for PSMA (Figure 3A). In this model, MEDI3726 showed a dose-dependent antitumor activity (Figure 3B), with an extended tumor stasis preceding regrowth after a single dose of 1 mg/kg, and a significant increase in the time-to-endpoint (TTE) survival, compared with all other groups (Supplementary Table S1). Additionally, MEDI3726 was associated with a statistically significant increase in animal survival, compared with the naked antibody group, at 0.33 mg/kg and 1 mg/kg (Supplementary Table S1). The non-targeting isotype control ADC was also associated with a statistical increase in survival compared with the control groups, but only at the highest dose of 1 mg/kg (Supplementary Figure S2 and Table S1).

Next, we investigated MEDI3726 in CWR22Rv1 xenografts, castration-resistant model (28). IHC analysis of the CWR22Rv1 xenograft tumors confirmed the heterogeneous expression of PSMA in this model, with approximately 20% to 50% of tumor cells staining positive for PSMA (Figure 3C, Supplementary Table S2). Administration of MEDI3726 resulted in a dose-dependent antitumor activity (Figure 3D), with a prolonged tumor regression (approximately 50 days) after a single 1 mg/kg dose (Supplementary Table S3). A single dose of the isotype control ADC at 0.75 mg/kg resulted in tumor growth comparable with that seen in vehicle-treated animals (Supplementary Figure S3). Notably, two monomethyl auristatin E-based, PSMA-targeted ADCs, PSMA-ADC1-MMAE (DAR = 4) and PSMA-ADC2-MMAE (DAR = 4), did not show antitumor activity at 3 mg/kg or 6 mg/kg. Nor did these ADCs show in vitro cytotoxic activity in CWR22Rv1 cells, although they did bind to PSMA positive cells and showed strong cytotoxic activity on LNCaP cells (Supplementary Figure S4).

In the PC-3 xenograft model, which did not express PSMA (Figure 3E), administration of MEDI3726 and the isotype control ADC resulted in limited antitumor activity at the highest dose (1 mg/kg) (Figure 3F, Supplementary Table S4). This result might have occurred because of non-target–specific uptake of the ADCs by the tumor cells and/or local release of PBD toxin caused by tumor associated macrophages (32).

In vivo activity of MEDI3726 in LuCaP prostate cancer PDX models

To further characterize the in vivo activity of MEDI3726, we assessed the efficacy of MEDI3726 against a panel of clinically relevant LuCaP prostate cancer PDX models. Among eight LuCaP models, six (LuCaP 70, 73, 77, 86.2, 96CR, 147) showed strong membrane expression of PSMA in more than 75% of tumor cells, as determined by IHC (Figure 4A and Supplementary Table S2). Of the remaining two, LuCaP 58 showed moderate PSMA staining intensity in 10% to 25% of tumor cells and LuCaP 35CR was negative for PSMA. Consistent with the results in the cell line xenografts, highly PSMA-positive LuCaP models responded in a dose-dependent manner to MEDI3726 (Figure 4, Panels B-G). Compared with untreated controls, animals treated with 0.9 mg/kg MEDI3726 showed statistically significant responses in all highly PSMA-positive LuCaP models. Complete and durable tumor regressions were observed in five of the six highly PSMA-positive models (Figure 4 Panels B-F). The LuCaP 147 model displayed a tumor regression

followed by a prolonged tumor stasis (Figure 4 Panel G). In the LuCaP 70, 73, and 96CR models, animals given 0.3 mg/kg MEDI3726 showed statistically significant tumor regressions compared with the untreated control group (Figure 4 Panels B, C and F). At this same dose, the LuCaP 77 model displayed a statistically significant prolonged tumor stasis (Figure 4 Panel D). In contrast, the 0.3 mg/kg dose of MEDI3726 only inhibited tumor growth in the LuCap 86.2 and 147 models (Figure 4 Panels E and G). The 0.1 mg/kg dose of MEDI3726 did not significantly delay tumor growth, compared with the control in any of the highly PSMA-positive LuCaP models. MED3726 was not associated with tumor growth inhibition at any dose in the heterogeneously PSMA-positive LuCaP 58 model or the PSMA-negative LuCap 35CR models (Figure 4 Panels H and I).

Next, we sought to investigate the phosphorylation of Histone H2AX (γ-H2AX), which occurs following the DNA damage induced by SG3199-generated ICLs. Tumors were collected from the LuCaP 73 xenograft bearing mice 48 hours after the first single administration of each ADC. A dose-related increase in the number of γ-H2AX-positive nuclei was observed among each of the MEDI3726 treatment groups, compared with both the control and isotype control groups. However, statistical significance was achieved only at the highest MEDI3726 dose tested (Figure 4J and Supplementary Figure S5). It is important to note that the collection time point at 48 hours post single dose may not have been optimal to detect the differences in γ-H2AX positive cells between the two lower dose levels, given that the tumor regression was not observed until the second dose of 0.3 mg/kg of MEDI3726.

MEDI3726 related toxicity, as determined by body weight measurements, was not observed in any of the cell line xenograft and PDX model studies (Supplementary Figure S6). As noted earlier, MEDI3726 does not bind to rodent PSMA.

Toxicology of MEDI3726 in Cynomolgus Monkey

Cynomolgus monkey was selected as a relevant species for the toxicity study after MEDI3726 demonstrated comparable cross-reactive binding activity to human and cynomolgus monkey PSMA as determined by BIAcore (SPR) and competitive ELISA assays (Table 1). A repeat-

dose, good-laboratory-practice (GLP) toxicology study of MEDI3726 was assessed in cynomolgus monkeys (5/sex/group) which were administered IV injections of 0.15, 0.3 or 0.6 mg/kg MEDI3726 on days 1 and/or 22. Animals were necropsied on days 29 (main study; 3/sex/group) and 71 (recovery; 2/sex/group).

No changes were noted in body weight, blood clinical chemistry, urine, coagulation parameters, body temperature, physical and neurological exams, neurobehavior, ophthalmology, cardiovascular end-points (electrocardiogram [ECG] and blood pressure), respiratory rate or organ weights.

Dose-dependent reversible myelosuppression was the primary toxicity, correlating with reversible findings in the bone marrow (hypocellularity of erythroid and myeloid cells and megakaryocytes) and transient neutropenia (Supplementary Figure S7). Dose-dependent (late onset) reversible black skin discoloration, correlating with epidermal hyperpigmentation and hyperplasia was observed as well as reversible microscopic changes in lymphoid organs (decreased or absent germinal centers) and kidney (tubular degeneration, cellular hypertrophy/atypia, focal inflammation, and edema). Changes in the testis (seminiferous tubule degeneration, vacuolation, reduced sertoli cells and loss of germ cells) were not fully recoverable during the study, but the presence of intact spermatogonia in the testis supported that full recovery would be evident with time (33). The Highest Non-Severely Toxic Dose (HNSTD), was the highest dose tested of 0.6 mg/kg.

DISCUSSION

MEDI3726 is a PSMA-targeting ADC generated via site-specific conjugation of an engineered version of the J591 antibody to the PBD-based linker-drug tesirine. In vitro, MEDI3726 demonstrated potent and specific cytotoxic activity. In the CWR22Rv1 cell line, where approximately 40% of the cells were positive for PSMA expression, MEDI3726 demonstrated potent in vitro activity, with close to 100% of the cells being killed. This maximum cell kill was likely achieved via bystander activity, which has been reported for other ADCs using tesirine (27,34,35). In agreement with the potent in vitro activity observed with the CWR22Rv1 cell line,

durable tumor regressions was observed after a single MEDI3726 dose administration to mice subcutaneously implanted with the CWR22Rv1 cells. Thus, both in vitro and in vivo data suggest that MEDI3726 has robust bystander activity with an ability to kill neighboring non-PSMA expressing tumor cells. Interestingly, MEDI3726 demonstrated a more potent activity in the CWR22Rv1 xenograft study compared to the LNCaP model even though the LNCaP model had more intense and homogeneous PSMA expression. Many factors may explain this observation. For example, difference in the tumor stromal component could impact the ADC perfusion or the high, homogeneous PSMA expression found in LNCaP tumor cells could potentially prevent a more efficient tumor penetration and distribution due to the "binding site barrier" effect (36). Imaging studies investigating the tumor distribution of MEDI3726 may help us understand the differences in efficacy between these two models. Importantly, multiple doses of two auristatin-based PSMA-ADCs (US 8114965 B2) (3 mg/kg or 6 mg/kg, q4d x 6) did not result in any significant antitumor activity in the CWR22Rv1 xenograft model.

PDX models were used to assess the in vivo activity of MEDI3726. Such models are particularly important for assessing in vivo activity in prostate cancer, for which the number of available cell line xenograft models is limited. LuCaP PDX models have been derived from patient samples at various stages of disease and metastatic sites, and thus reflect the genetic and phenotypic heterogeneity of the disease (29). MEDI3726-responsive models represented various types of castration-resistant prostate cancer (LuCaP 70, 73, 77, 86.2, 96CR, 147) and metastasis (LuCaP 70, 77, 86.2, and 147). MEDI3726-responsive models also varied in AR expression; AR gain-of-function mutations (present in LuCaP 73 and 147) and the splice variants ARV7 (31) and AR-V567es (present in LuCaP 86.2) (30) which have been implicated in the resistance to AR inhibitors. Moreover, MEDI3726 appeared more potent compared to the auristatin based PSMA-ADC, as a lower dose and less frequent administration showed comparable to superior anti-tumor activity in LuCaP 96CR and LuCaP 77 PDX models, respectively, in comparison to the published auristatin PSMA ADC results in the these models (37). Interestingly, MEDI3726 had minimal antitumor activity in the LuCaP 58 model, which like CWR22Rv1 showed heterogeneous PSMA expression. The difference in anti-tumor activity may have been due to fewer PSMA-positive tumor cells in the LuCaP 58 model compared to the CWR22Rv1 model.

As part of the Investigational New Drug Application enabling studies, MEDI3726 was tested in a repeat-dose, intravenous, GLP study in cynomolgus monkeys. The major adverse effects following administration of MEDI3726 were related primarily to the known safety profile previously reported in a phase 1 study of an ADC containing the same linker-drug teserine (38) and were consistent with the profile associated with the mechanism of action of the PBD dimer warhead. The major dose-limiting toxicity associated with MEDI3726 was myelosuppression, but this effect was readily monitorable. Overall, the toxicology profile of MEDI3726 supported further study of the drug in phase 1 clinical trials.

PSMA is a well-characterized tumor associated antigen for prostate cancer and possesses many features that make it attractive for an ADC-mediated targeting approach to mCRPC. Two PSMA-targeting ADCs using tubulin-inhibiting payloads have been investigated in clinical studies in patients with mCRPC (16,39). MLN2704, an ADC utilizing the unmodified J591 anti-PSMA antibody, has shown a limited therapeutic window in a Phase 1/2 study in mCPRC patients attributed to the unstable disulfide linker, leading to rapid deconjugation of the DM1 warhead after administration to patients (39). PSMA ADC has demonstrated anti-tumor activity in a Phase 2 study in patients with mCRPC based on radiological response and reductions in circulating tumor cells and prostate-specific antigen (16). While neither of these tubulin inhibitor based ADCs is under current clinical development, MEDI3726 is the first PSMA targeting ADC utilizing the highly potent DNA crosslinking PBD payload tesirine in clinical development for mCRPC (NCT02991911).

Preclinical studies have demonstrated that reduced expression of BRCA1 or BRCA2, key components of the homologous recombination (HR) pathway involved in the repair of PBD mediated DNA damage, increases the sensitivity of tumor cells to PBD-mediated cell death (40,41). Notably, recent data have shown that mutations in DNA repair pathway genes occur in 20% to 25% of prostate cancer cases (42). Thus, disruption in DNA repair pathway in prostate cancer may make difficult to treat tumors such as mCRPC especially sensitive to DNA damaging PBD payloads compared to the microtubule-inhibitor based ADCs previously studied in clinical trials. Moreover, pharmacological suppression of the AR pathway not only increases the

expression of PSMA, but also decreases the expression of genes involved in the HR pathway (43,44).

In conclusion, the emerging data showing frequent mutations of DNA damage response (DDR) genes in prostate cancer together with the decreased DDR gene expression induced by pharmacological suppression of the AR pathway provide a strong rationale for targeting prostate cancer with MEDI3726, which combines specific targeting of highly expressed prostate cancer tumor antigen PSMA with a potent DNA damage inducer, not only as monotherapy, but also in conjunction with AR pathway inhibitors.

Acknowledgments

This study was supported by MedImmune, the global biologic R&D arm of AstraZeneca. The authors would like to thank Dr. Barry R. Davies, and Ms. Holly Nguyen for the input and support in selecting and establishing LuCaP models at MedImmune. In addition, we thank Dr. David W. Jenkins for contributions in the preclinical development of MEDI3726 and Dr. Rakesh Dixit for the critical review of the manuscript. Editorial support was provided by Frances McFarland, PhD, MA (funded by MedImmune).

References

1. Siegel RL, Miller KD, Jemal A. Cancer Statistics, 2017. CA Cancer J Clin 2017;67(1):7-30.
2. Feldman BJ, Feldman D. The development of androgen-independent prostate cancer. Nat Rev Cancer 2001;1(1):34-45.
3. Antonarakis ES, Lu C, Wang H, Luber B, Nakazawa M, Roeser JC, et al. AR-V7 and resistance to enzalutamide and abiraterone in prostate cancer. N Engl J Med 2014;371:1028-38.
4. Ristau BT, O'Keefe DS, Bacich DJ. The prostate-specific membrane antigen: lessons and current clinical implications from 20 years of research. Urol Oncol 2014;32:272-9.
5. Tagawa ST, Beltran H, Vallabhajosula S, Goldsmith SJ, Osborne J, Matulich D, et al. Anti-prostate-specific membrane antigen-based radioimmunotherapy for prostate cancer. Cancer 2010;116(4 Suppl):1075-83.
6. Israeli RS, Powell CT, Corr JG, Fair WR, Heston WD. Expression of the prostate-specific membrane antigen. Cancer Res 1994;54:1807-11.
7. Silver DA, Pellicer I, Fair WR, Heston WD, Cordon-Cardo C. Prostate-specific membrane antigen expression in normal and malignant human tissues. Clin Cancer Res 1997;3:81-5.
8. Tsourlakis MC, Klein F, Kluth M, Quaas A, Graefen M, Haese A, et al. PSMA expression is highly homogenous in primary prostate cancer. Appl Immunohistochem Mol Morphol 2015;23(6):449-55.
9. Wright GL, Jr., Grob BM, Haley C, Grossman K, Newhall K, Petrylak D, et al. Upregulation of prostate-specific membrane antigen after androgen-deprivation therapy. Urology 1996;48:326-34.
10. Chang SS, Reuter VE, Heston WD, Bander NH, Grauer LS, Gaudin PB. Five different anti-prostate-specific membrane antigen (PSMA) antibodies confirm PSMA expression in tumor-associated neovasculature. Cancer Res 1999;59(13):3192-8.
11. Haffner MC, Kronberger IE, Ross JS, Sheehan CE, Zitt M, Muhlmann G, et al. Prostate-specific membrane antigen expression in the neovasculature of gastric and colorectal cancers. Hum Pathol 2009;40:1754-61.

12. Vallabhajosula S, Nikolopoulou A, Jhanwar YS, Kaur G, Tagawa ST, Nanus DM, et al. Radioimmunotherapy of Metastatic Prostate Cancer with (1)(7)(7)Lu-DOTAhuJ591 Anti Prostate Specific Membrane Antigen Specific Monoclonal Antibody. Curr Radiopharm 2016;9:44-53.
13. Von Hoff DD, Mita MM, Ramanathan RK, Weiss GJ, Mita AC, LoRusso PM, et al. Phase I Study of PSMA-Targeted Docetaxel-Containing Nanoparticle BIND-014 in Patients with Advanced Solid Tumors. Clin Cancer Res 2016;22:3157-63.
14. Friedrich M, Raum T, Lutterbuese R, Voelkel M, Deegen P, Rau D, et al. Regression of human prostate cancer xenografts in mice by AMG 212/BAY2010112, a novel PSMA/CD3-Bispecific BiTE antibody cross-reactive with non-human primate antigens. Mol Cancer Ther 2012;11:2664-73.
15. Tagawa ST, Milowsky MI, Morris M, Vallabhajosula S, Christos P, Akhtar NH, et al. Phase II study of Lutetium-177-labeled anti-prostate-specific membrane antigen monoclonal antibody J591 for metastatic castration-resistant prostate cancer. Clin Cancer Res 2013;19:5182-91.
16. Petrylak DP, Vogelzang NJ, Chatta GS, Fleming MT, Smith DC, Appleman LJ, et al. A phase 2 study of prostate specific membrane antigen antibody drug conjugate (PSMA ADC) in patients (pts) with progressive metastatic castration-resistant prostate cancer (mCRPC) following abiraterone and/or enzalutamide (abi/enz). Journal of Clinical Oncology 2015;33.
17. Mahalingam D, Wilding G, Denmeade S, Sarantopoulas J, Cosgrove D, Cetnar J, et al. Mipsagargin, a novel thapsigargin-based PSMA-activated prodrug: results of a first-in-man phase I clinical trial in patients with refractory, advanced or metastatic solid tumours. Br J Cancer 2016;114:986-94 doi.
18. Kiess AP, Banerjee SR, Mease RC, Rowe SP, Rao A, Foss CA, et al. Prostate-specific membrane antigen as a target for cancer imaging and therapy. Q J Nucl Med Mol Imaging 2015;59:241-68.
19. Sievers EL, Senter PD. Antibody-drug conjugates in cancer therapy. Annu Rev Med 2013;64:15-29.
20. Hartley JA. The development of pyrrolobenzodiazepines as antitumour agents. Expert Opin Investig Drugs 2011;20:733-44.

21. Adair JR, Howard PW, Hartley JA, Williams DG, Chester KA. Antibody-drug conjugates - a perfect synergy. Expert Opin Biol Ther 2012;12:1191-206.
22. Beck A, Goetsch L, Dumontet C, Corvaia N. Strategies and challenges for the next generation of antibody-drug conjugates. Nat Rev Drug Discov 2017;16(5):315-37.
23. Hamilton A, King S, Liu H, Moy P, Bander N, Carr F. A novel humanized antibody against prostate specific membrane antigen (PSMA) for in vivo targeting and therapy. Proc Am Assoc Cancer Res 1998;39:440.
24. Tiberghien AC, Levy JN, Masterson LA, Patel NV, Adams LR, Corbett S, et al. Design and Synthesis of Tesirine, a Clinical Antibody-Drug Conjugate Pyrrolobenzodiazepine Dimer Payload. ACS Med Chem Lett 2016;7:983-7.
25. Edelman GM, Cunningham BA, Gall WE, Gottlieb PD, Rutishauser U, Waxdal MJ. The covalent structure of an entire gammaG immunoglobulin molecule. Proc Natl Acad Sci U S A 1969;63:78-85.
26. Hartley JM, Spanswick VJ, Hartley JA. Measurement of DNA damage in individual cells using the Single Cell Gel Electrophoresis (Comet) assay. Methods Mol Biol 2011;731:309-20.
27. Flynn MJ, Zammarchi F, Tyrer PC, Akarca AU, Janghra N, Britten CE, et al. ADCT-301, a Pyrrolobenzodiazepine (PBD) Dimer-Containing Antibody-Drug Conjugate (ADC) Targeting CD25-Expressing Hematological Malignancies. Mol Cancer Ther 2016;15:2709-21.
28. Sramkoski RM, Pretlow TG, 2nd, Giaconia JM, Pretlow TP, Schwartz S, Sy MS, et al. A new human prostate carcinoma cell line, 22Rv1. In Vitro Cell Dev Biol Anim 1999;35:403-9.
29. Nguyen HM, Vessella RL, Morrissey C, Brown LG, Coleman IM, Higano CS, et al. LuCaP Prostate Cancer Patient-Derived Xenografts Reflect the Molecular Heterogeneity of Advanced Disease and Serve as Models for Evaluating Cancer Therapeutics. Prostate 2017;77:654-71.
30. Sun S, Sprenger CC, Vessella RL, Haugk K, Soriano K, Mostaghel EA, et al. Castration resistance in human prostate cancer is conferred by a frequently occurring androgen receptor splice variant. The Journal of clinical investigation 2010;120:2715-30.

31. DiPippo VA, Nguyen HM, Brown LG, Olson WC, Vessella RL, Corey E. Addition of PSMA ADC to enzalutamide therapy significantly improves survival in in vivo model of castration resistant prostate cancer. Prostate 2016;76:325-34.
32. Li F, Ulrich M, Jonas M, Stone IJ, Linares G, Zhang X, et al. Tumor-Associated Macrophages Can Contribute to Antitumor Activity through FcgammaR-Mediated Processing of Antibody-Drug Conjugates. Mol Cancer Ther 2017;16:1347-54.
33. Dreef HC, Van Esch E, De Rijk EP. Spermatogenesis in the cynomolgus monkey (Macaca fascicularis): a practical guide for routine morphological staging. Toxicol Pathol. 2007;35:395-404.
34. Zammarchi F, Chivers S, Williams DG, Adams L, Mellinas-Gomez M, Tyrer P, et al. ADCT-502, a novel pyrrolobenzodiazepine (PBD)-based antibody-drug conjugate (ADC) targeting low HER2-expressing solid cancers. Eur J Cancer 2016;69:S28-S.
35. Zammarchi F, Williams DG, Adams L, Havenith K, Chivers S, D'Hooge F, et al. Pre-Clinical Development of Adct-402, a Novel Pyrrolobenzodiazepine (PBD)-Based Antibody Drug Conjugate (ADC) Targeting CD19-Expressing B-Cell Malignancies. Blood 2015;126.
36. Fujimori K, Covell DG, Fletcher JE, Weinstein JN. Modeling analysis of the global and microscopic distribution of immunoglobulin G, F(ab')2, and Fab in tumors. Cancer Res 1989;49:5656-63.
37. DiPippo VA, Olson WC, Nguyen HM, Brown LG, Vessella RL, Corey E. Efficacy studies of an antibody-drug conjugate PSMA-ADC in patient-derived prostate cancer xenografts. Prostate 2015;75:303-13.
38. Rudin CM, Pietanza MC, Bauer TM, Ready N, Morgensztern D, Glisson BS, et al. Rovalpituzumab tesirine, a DLL3-targeted antibody-drug conjugate, in recurrent small-cell lung cancer: a first-in-human, first-in-class, open-label, phase 1 study. Lancet Oncol 2017;18:42-51.
39. Milowsky MI, Galsky MD, Morris MJ, Crona DJ, George DJ, Dreicer R, et al. Phase 1/2 multiple ascending dose trial of the prostate-specific membrane antigen-targeted antibody drug conjugate MLN2704 in metastatic castration-resistant prostate cancer. Urol Oncol 2016;34(12):530 e15- e21.

40. Hucl T, Rago C, Gallmeier E, Brody JR, Gorospe M, Kern SE. A syngeneic variance library for functional annotation of human variation: application to BRCA2. Cancer Res 2008;68:5023-30.

41. Zhong H, Tammali R, Chen C, Fazenbaker , Maureen K, Monks M, et al. Abstract 76: Synthetic lethal targeting of BRCA mutant tumors with antibody linked pyrrolobenzodiazepine dimers. Annual Meeting of the American Association for Cancer Research; April 1-5, 2017; Washington, DC.

42. Dhawan M, Ryan CJ, Ashworth A. DNA Repair Deficiency Is Common in Advanced Prostate Cancer: New Therapeutic Opportunities. Oncologist 2016;21:940-5.

43. Murga JD, Moorji SM, Han AQ, Magargal WW, DiPippo VA, Olson WC. Synergistic co-targeting of prostate-specific membrane antigen and androgen receptor in prostate cancer. Prostate 2015;75:242-54.

44. Li L, Karanika S, Yang G, Wang J, Park S, Broom BM, et al. Androgen receptor inhibitor-induced "BRCAness" and PARP inhibition are synthetically lethal for castration-resistant prostate cancer. Sci Signal 2017;10.

Author Manuscript Published OnlineFirst on July 31, 2018; DOI: 10.1158/1535-7163.MCT-17-0982
Author manuscripts have been peer reviewed and accepted for publication but have not yet been edited.

Table 1. Affinity and Species Cross-Reactivity of MEDI3726, as Determined by Competitive ELISA

EC_{50} ng/mL (95% CI) (ng/mL)	
Human sPSMA	17.92 (13.35 to 24.05)
Cynomolgus monkey sPSMA	16.89 (12.45 to 22.91)
Rat sPSMA	Does not compete
Surface Plasmon Resonance (K_D nM ± SD)	
Human sPSMA	1.67 ± 0.83
Cynomolgus monkey sPSMA	3.11 ± 0.19

Note: EC_{50}, half-maximal effective concentration; K_D, dissociation constant

Table 2. Summary of Cell Line Characterization and In Vitro Activity

Cell Lines	Flow Cytometry		Cytotoxic Activity		
	Antigen Density (± SEM)	% PSMA-positive Cells (± SEM)	SG3199 (IC50 nM ± SEM)	MEDI3726 (IC50 nM ± SEM)	Isotype Control ADC (IC50 nM ± SEM)
LNCaP	250,494 (1,229)	92 (5)	0.04 (0.01)	0.02 (0.003)	3.83 (1.01)
LNCaP C4-2	250,446 (2,251)	91 (8)	0.16 (0.02)	0.06 (0.01)	7.47 (0.45)
CWR22Rv1	43,776 (4,237)	40 (7)	0.07 (0.01)	0.29 (0.21)	3.56 (0.36)
MDA PCa2b	117,635 (5,200)	95 (0)	1.05 (0.36)	0.002 (0.001)	0.51 (0.09)
PC3	Negative	NA	0.24 (0.10)	29.3 (0.6)	25.2 (1.55)
DU145	Negative	NA	0.26 (0.06)	44.9 (7.7)	37.4 (8.33)

Note: The cytotoxicity of SG3199, MEDI3726, and the isotype control ADC was determined by CellTitreGlo assay. n = 3; NA = not applicable; Negative = below the lower limit of quantitation (7,348).

Figure Legends

Figure 1. Schematic of MEDI3726. The pyrrolobenzodiazepine is site-specifically conjugated to the antibody endogenous cysteine in the constant domain of the antibody heavy chain, resulting in a drug-to-antibody ratio close to 2.

Figure 2. Confocal Images of Internalization and Comet Assay Analysis of DNA Interstrand Crosslink Formation. PSMA-positive LNCaP (A) and PSMA-negative PC3 (B) cells were incubated for 24 h with MEDI3726 or the isotype control ADC (C and D). Representative images are shown: LAMP-1-positive lysosomes are red, MEDI3726 appears in green, and colocalization of MEDI3726 with LAMP-1 is shown in yellow. Results of the Comet assay are shown in LNCaP (E) and PC-3 cells (F), compared with irradiated control cells. Results are presented as mean % Olive Tail Moment ± SEM (n = 3).

Figure 3. In Vivo Activity of MEDI3726 in Prostate Cancer Xenograft Models. (A) PSMA IHC of LNCaP cells; (B) Male nude mice implanted with LNCaP cells in Matrigel were dosed once with the vehicle control, MEDI3726, isotype control ADC, or unconjugated antibody; (C) PSMA IHC of CWR22Rv1 cells; (D) Male SCID mice bearing CWR22Rv1 xenografts were dosed once with MEDI3726 or vehicle. MMAE-based PSMA-targeted ADCs, PSMA-ADC1-MMAE and PSMA-ADC2-MMAE, were administered once every 4 days for six doses. (E) PSMA IHC of PC-3 cells (F) Female athymic nude mice bearing PC-3 xenografts were dosed once with vehicle control, unconjugated antibody, MEDI3726, or isotype control ADC. In each in vivo study, data represent the mean tumor volume ± SEM (n = 10). IHC, immunohistochemistry; MMAE, monomethyl auristin E; qd × 1, once daily dosing for 1 day; qd × 4, dosing once every 4 days. Scale bars, 100 μm.

Figure 4. MEDI3726 inhibits tumor growth in PSMA expressing prostate cancer PDX models. (A) Shown are representative micrographs of the PSMA IHC of LuCaP tumor sections. Scale bars are 100 μm. Insets are images of respective whole xenograft sections. For the PDX in vivo study, dosing was initiated when tumor volumes reached 150 mm^3 to 250mm^3. (B) LuCaP 70($PSMA^{High}$), (C) LuCaP 73($PSMA^{High}$), (D) LuCaP 77($PSMA^{High}$), (E) LuCaP 86.2($PSMA^{High}$), (F) LuCaP 96CR($PSMA^{High}$), (G) LuCaP 147($PSMA^{High}$), (H) LuCaP 58($PSMA^{hetrogeneous}$) and (I) LuCaP 35CR($PSMA^{negative}$) were treated intravenously with MEDI3726 at 0.1 (▼), 0.3 (●) and 0.9 (◆) mg/kg, isotype control ADC at 0.9 (▲) mg/kg, or

vehicle (■) once every 3 weeks for three doses (q3w x 3). The vertical dotted lines indicate the days of treatment. Data shown are the group mean ± SEM of n = 6 animals/group. Statistical analysis of the in vivo tumor data was performed by ANOVA followed by Dunn's pairwise testing for raw data (Panels B and D), Dunnett's pairwise testing for raw data (Panels H and I), or log10 transformed data (Panels C, E, F and G). **P* <0.05; ***P* <0.01; ****P* < 0.001 (J) LuCaP 73 xenograft bearing animals were dosed once and xenograft tumors collected 48 hours post dose for γ-H2AX IHC. Percent γ-H2AX-positive nuclei. *****P* < 0.0001 (ANOVA post-hoc Tukey for multiple comparison) for the group given the 0.9-mg/kg MEDI3726 dose, compared with all other groups. Error bars, SD; n ≥ 2.

Figure 1

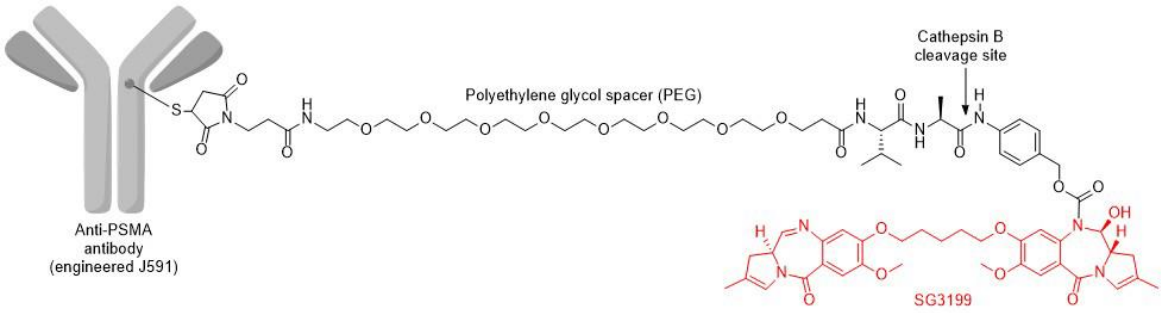

Figure 2

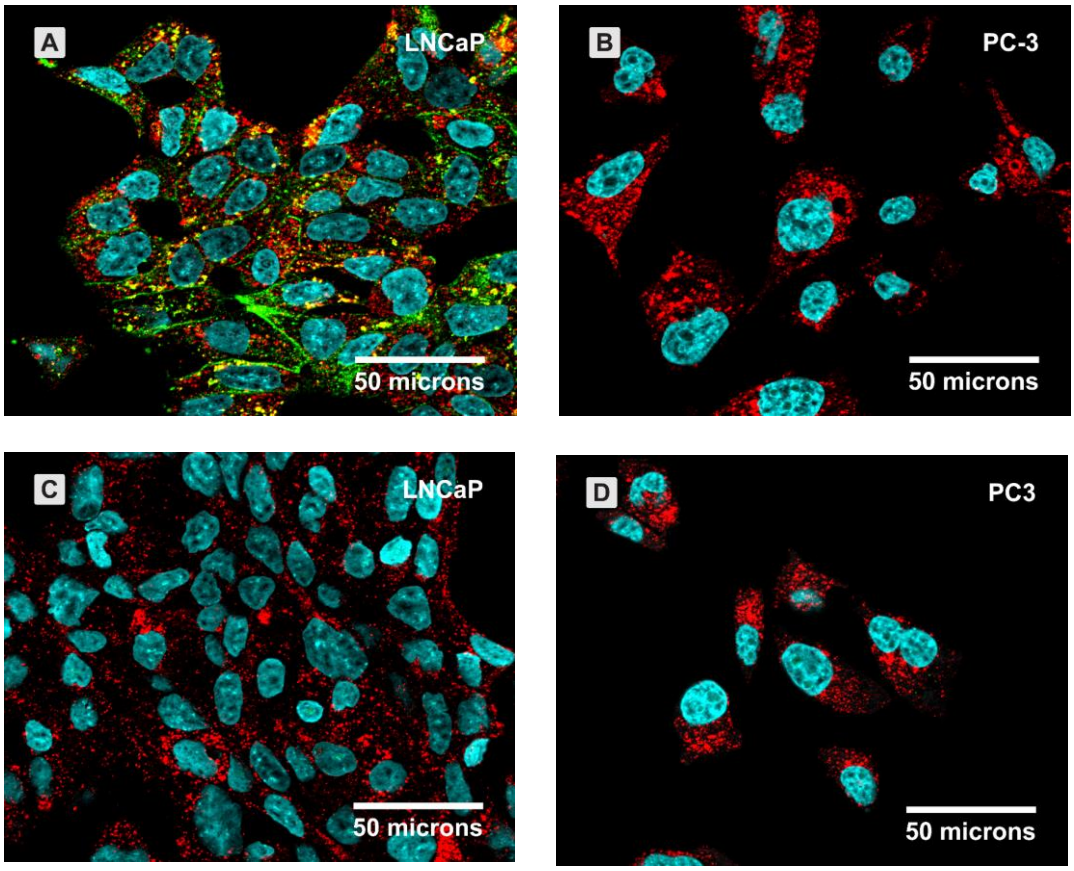

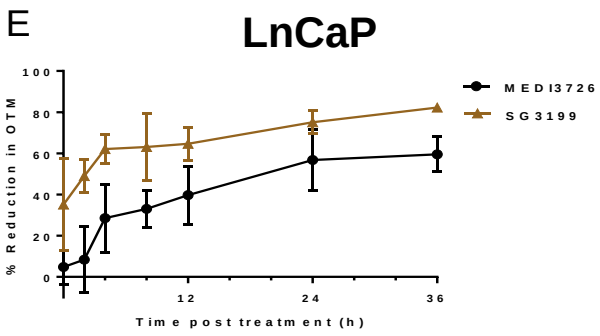

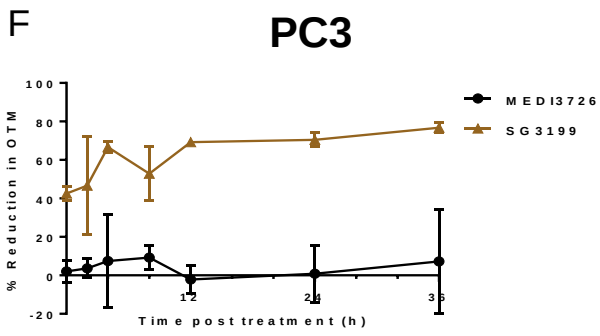

Figure 3

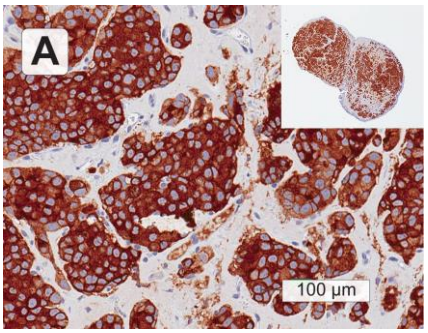

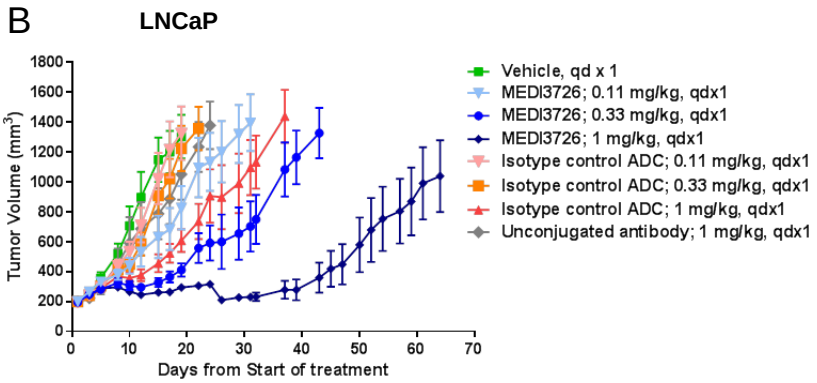

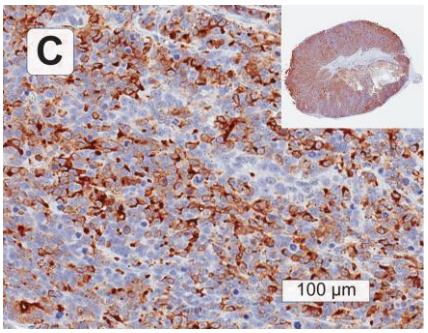

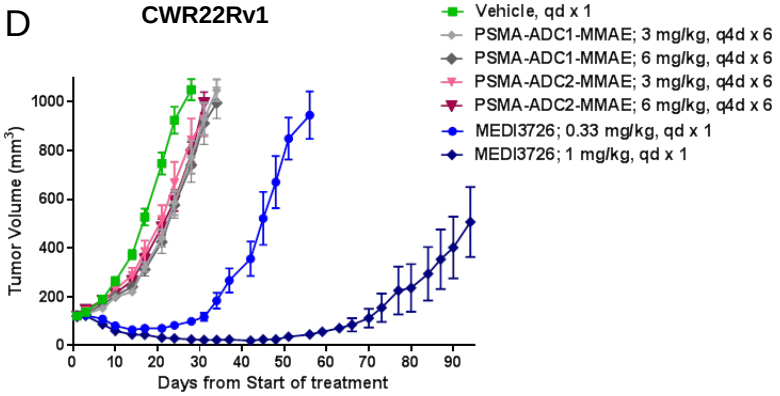

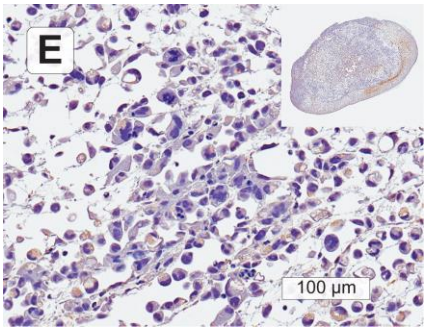

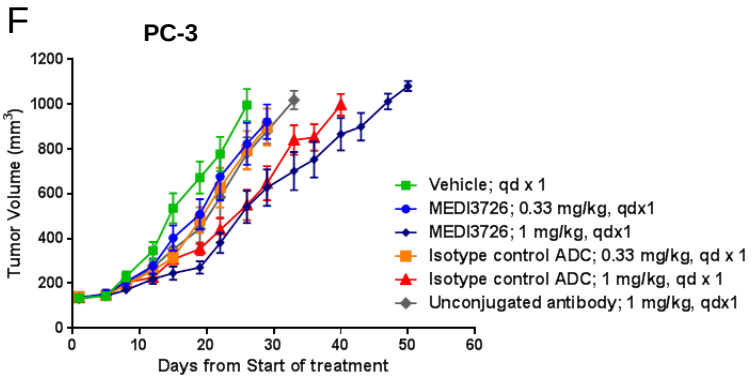

Figure 4

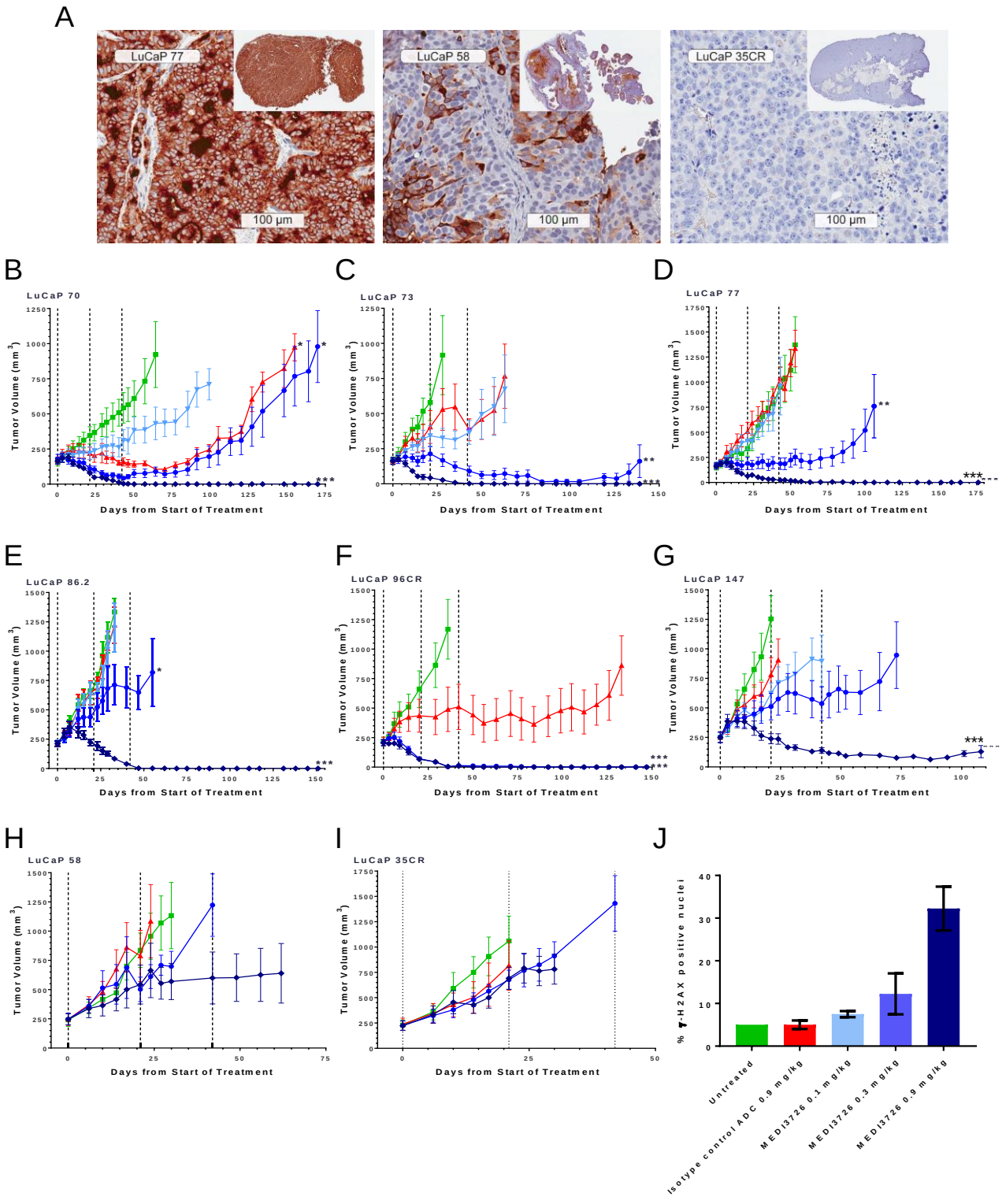

AACR American Association for Cancer Research

Molecular Cancer Therapeutics

Antitumor Activity of MEDI3726 (ADCT-401), a Pyrrolobenzodiazepine Antibody-drug Conjugate Targeting PSMA, in Pre-clinical Models of Prostate Cancer

Song Cho, Francesca Zammarchi, David G Williams, et al.

Mol Cancer Ther Published OnlineFirst July 31, 2018.